A R C H I V E S O F M E T A L L U R G Y A N D M A T E R I A L S
Volume 60 2015 Issue 2
DOI: 10.1515/amm-2015-0116

J.-K. KIM*, H.M. SHIM*, M.-J. PARK**, K.-K. KOO**,♯

FORMATION AND STABILIZATION OF SILVER NANOPARTICLES IN ETHANOL BY PHOSPHINIC ACID

REDUKCJA I STABILIZACJA NANOCZĄSTEK SREBRA W ETANOLU PRZEZ KWAS FOSFOROWY

Although phosphinic acid (H_3PO_2) has a powerful reduction potential, the reduction of silver ions by phosphinic acid salt has not yet been reported. In this work, colloidal silver has successfully synthesized by reducing silver ions in ethanol with phosphinic acid as a reducing agent. The effects of $[AgNO_3]/[H_3PO_2]$ ratios and reaction temperature were considered. Spherical silver nanoparticles with cubic structure were successfully prepared and their diameters were measured to be 8.5±0.9 nm - 11.3±0.2 nm. Half-life analysis showed that the reduction of silver ions proceeded with the reaction order of 1.30 on concentration of phosphinic acid and activation energy of 120.7 kJ/mol.

Keywords: Silver, nanoparticle, kinetic analysis, phosphinic acid, reduction

1. Introduction

Over the past decades, silver nanoparticles have surfaced due to their special physico-chemical properties and wide applications in photography, catalyst, surface-enhanced Raman scattering (SERS) detection, molecular sensors, antibacterial agents, conductive pastes and inks [1-5]. Numerous chemical reduction methods including polyol, microemulsion, seed-mediated growth and biological synthesis have been attempted to prepare the silver nanoparticles. Stabilizers, reducing agents, and silver salts are key components in reduction of the silver ions. Formaldehyde, hydrazine, sodium borohydride, L-ascorbic acid, polyols and sugars generally silver ions in either aqueous or organic phase. Starch, cyclodextrin, gelatin, gum Arabic, methylcellulose, L-gluthathione, poly (vinylpyrrolidone) (PVP) and poly (vinyl alcohol) (PVA) are a common stabilizer to disperse the silver particles in aqueous or organic medium [6-12]. Among many techniques to prepare nano-sized silver particles, wet reduction is probably the most popular one due to simplicity, easy operation and cost-efficient. The dispersion stability, shape, size and morphology of the silver nanoparticles depend on the reactants, reactant concentrations, reaction time, reaction medium, stabilizers, and temperatures. PVP would be one of the well-known stabilizer to disperse colloidal silver particles. PVP is a homopolymer consisting with vinyl structure and pyrrolidone containing a polar amide group with hydrophilic and electron-donating properties. In case of silver nanoparticles, the protective mechanism of PVP initially started from either the donation of the lone electrons of the pyrrolidyl nitrogen to silver particles or coordination bond between N in PVP and Ag [11-15]. Hydrazine (N_2H_4) and sodium borohydride ($NaBH_4$) are the strongest agents to reduce various metallic ions due to high redox potentials in alkaline pH. Although the phosphinic acid has a higher potential with hydrazine and sodium borohydride, reduction of common metal ions and the synthesis of the colloidal metal powders are rare except for nickel electroplating processes [16].

In this work, the stable silver colloids are prepared by reduction of silver nitrate by phosphinic acid as a reducing agent in the presence of PVP. Experimental variables are temperatures, mass ratios of silver ions and phosphinic acid. In-situ UV-VIS measurements of the silver colloids provide the vital information on the reduction kinetics of the silver ions via acquisition of the absorbance change with time. The average diameter, crystalline structure and their morphology of silver nanoparticles are investigated by using transmission electron microscopy (TEM) and X-ray diffractometry (XRD).

2. Experimental

Silver nitrate (99.8%, EP grade) and ethanol (99.5%, EP grade) were purchased from Samchun Pure Chemical Co. Ltd. Aqueous phosphinic acid (50%, EP grade) and PVP were purchased from Junsei Chemical Co. Ltd. Silver colloids were prepared by simple mixing together the silver nitrate/ethanol solution with aqueous phosphinic acid. In all experiments, concentrations of silver nitrate, phosphinic acid and PVP in ethanol were $5.0 \cdot 10^{-3}$ M. In a typical experiment, 3.2 cm^3 of $AgNO_3$ solution was heated to 25°C – 35°C. The most reactions were ended within 10 h. Ultraviolet-Visible (UV-VIS) spectra of silver colloids were recorded at 10 mm optical quartz cuvettes (Sarstedt, Germany) agitated with a magnetic

* SOGANG UNIVERSITY, SEOUL, REPUBLIC OF KOREA
♯ Corresponding author: koo@sogang.ac.kr

stirrer within 300 nm – 700 nm and averaged with 10 times using an S-3150 spectrophotometer (Scinco. Co. Ltd, Korea). Silver-free ethanolic PVP solutions containing aqueous phosphinic acid was a blank sample for background elimination in all experiments. Transmission electron microphotographs (TEM) were obtained from a Philips Tecnai F20 operating at 200 kV to observe silver nanoparticles. The average particle size of silver nanoparticles was calculated by image analysis of TEM microphotographs, counted up to at least 100 particles. XRD analysis of the colloidal silver was made by Miniflex (Rigaku, Japan) operating at a voltage of 30 kV and a current of 15 A with Cu K alpha radiation.

3. Results and discussion

3.1. Synthesis of silver colloids

Figure 1 shows TEM microphotographs taken to observe the shape and the average diameter of the silver nanoparticles prepared at different mass ratios of $AgNO_3$ and H_3PO_2 at 25°C. Mass ratio of PVP and $AgNO_3$ was 1:1. It is shown that spherical silver nanoparticles were formed with average diameter of 9.4±0.4 nm, 11.3±0.1 nm, 11.3±0.2 nm. As H_3PO_2 concentrations increased, the mean diameter of the silver nanoparticles was slightly increased, but the were not changed.

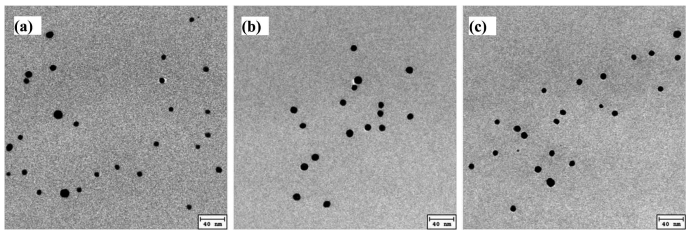

Fig. 1. TEM microphotographs of the Ag nanoparticles prepared at various mass ratios of $AgNO_3$ and H_3PO_2: (a) 1:1, (b) 1:2, (c), 1:4. Reaction condition: $AgNO_3$:PVP = 1:1, T= 25°C

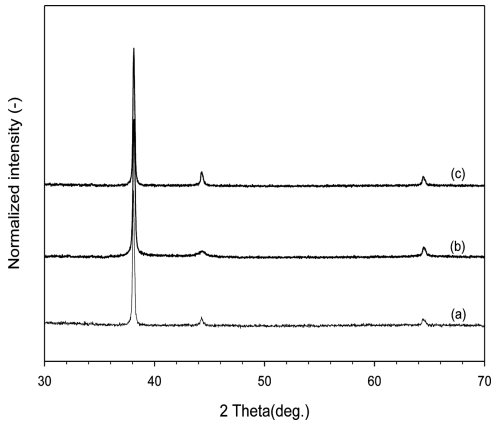

Fig. 2. XRD patterns of silver nanoparticles prepared at various ratios of $AgNO_3$ and H_3PO_2: (a) 1:1, (b) 1:2, (c), 1:4. Reaction condition: $AgNO_3$:PVP = 1:1, T= 25°C

Fig. 2 represents the XRD patterns of the silver nanoparticles prepared at the same conditions given in Fig. 1. The diffraction peaks of silver nanoparticles, overlaid in Fig. 2, are 2θ = 38°, 44°, 65°, matched well with the standard patterns of face centered-cubic structure of crystalline silver (JCPDS No. 04-0783) [9].

Fig. 3 shows the TEM microphotographs of the silver nanoparticles synthesized at different temperatures. For 25°C, 30°C, and 35°C, the average diameters of silver nanoparticles were calculated to be 9.4±0.4 nm, 8.5±0.9 nm, and 9.2±0.8 nm, respectively. Decreasing temperatures induced the longer reaction time but was independent of the average diameter of silver nanoparticles. From Fig. 1 and Fig. 3, it is clear that temperature and reactant concentration affect slightly the average diameter of the silver nanoparticles, not shape.

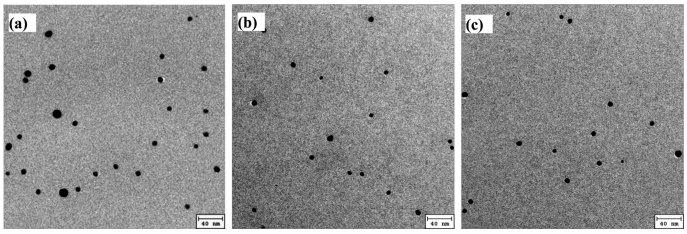

Fig. 3. TEM microphotographs of Ag nanoparticles prepared at various temperatures: (a) 25°C, (b) 30°C, (c) 35°C. Reaction condition: $AgNO_3$: PVP = 1:1, $AgNO_3$: H_3PO_2 = 1:1

Fig. 4 shows high-resolution TEM images of silver nanoparticles synthesized at 30°C and 35°C. In this figure, the crystal structure of silver nanoparticles appears without amorphous fractions. Planar disorders of silver nanoparticles including defects and dislocations are not shown. Thin layer, probably caused by PVP, adsorption was not observed. In Fig. 5, the formation of silver nanoparticles was directly identified by appearance of a strong sharp plasmon band at the wavelength of maximum absorbance λ_{max} = 390 nm – 422 nm. Within 10 h, the absorbances of the optical spectra were almost constant for all ratios of $AgNO_3$ and H_3PO_2. With reaction time, the resonance positions, λ_{max}, are shown to slightly move from 412 nm – 422 nm to 399 nm – 406 nm. In Fig.5, addition of more phosphinic acid solution shortened the reduction time of the silver ions but did not much change the absorbance of the silver colloids.

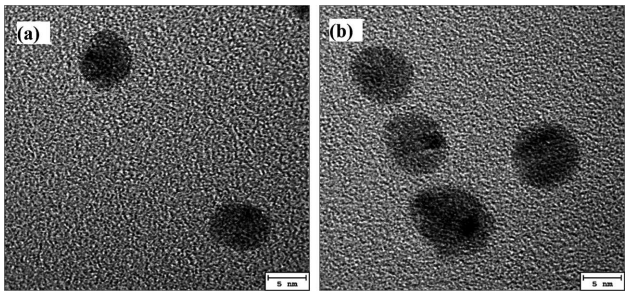

Fig. 4. High Resolution TEM microphotographs of Ag nanoparticles prepared at various temperatures: (a) 30°C, (b) 35°C. Reaction condition: $AgNO_3$: PVP = 1:1, $AgNO_3$: H_3PO_2 = 1:1

Full width at half maximum (FWHM) of UV-VIS spectra was calculated by Lorentzian fitting and background subtraction. With reaction time, FWHM was shown to become narrow and the peak positions of wavelength to be shorter. In all UV-VIS spectra, an interesting is no shoulder peaks near the plasmon bands. These results indicate that further growth and morphological changes of sil-

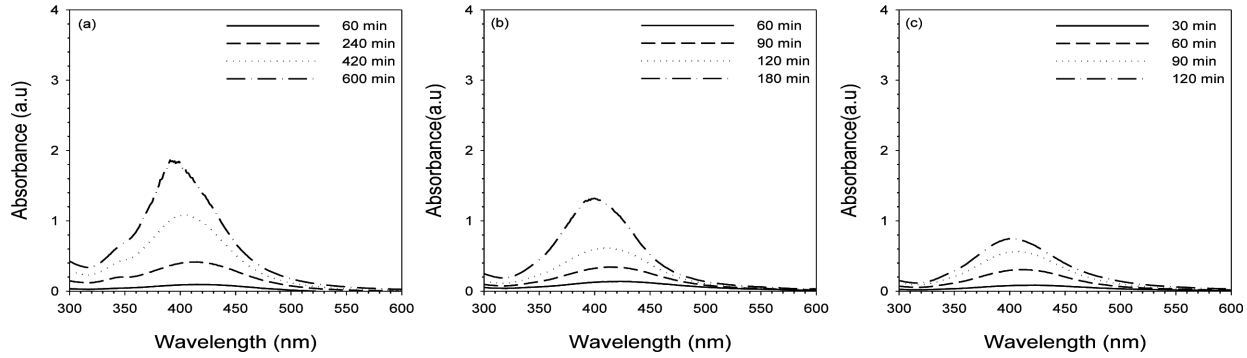

Fig. 5. Change of the UV absorbance with time at various mass ratios of $AgNO_3$ and H_3PO_2: (a) 1:1, (b) 1:2, (c) 1:4. Reaction condition: $AgNO_3$:PVP = 1:1, T= 25°C

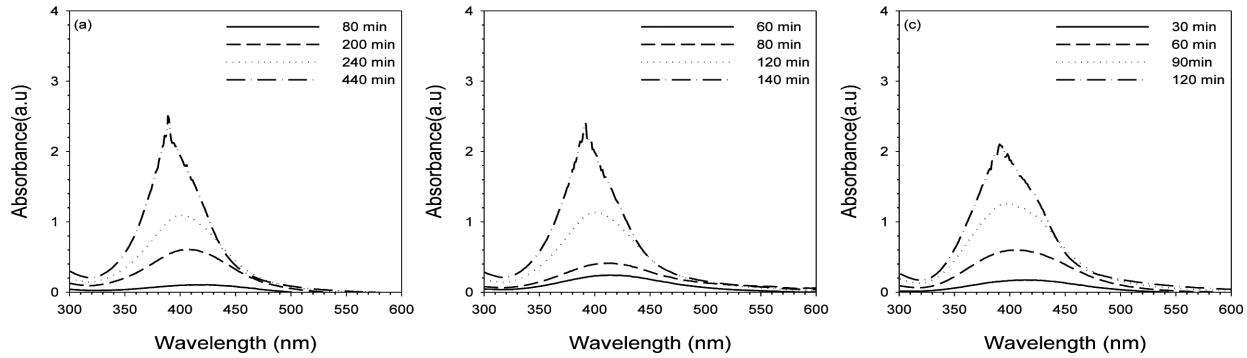

Fig. 6. Change of the UV absorbance with time at various temperatures: (a) 25°C, (b) 30°C, (c) 35°C. Reaction condition: $AgNO_3$: PVP = 1:1, $AgNO_3$: H_3PO_2 = 1:1

ver nanoparticles were not occurred. Similar observations were made at the UV-VIS absorption spectra of silver colloids prepared at various reaction temperatures in Fig. 6.

FWHM broadening of the silver colloids could be explained by the following reasons. As shown in Fig. 1 and Fig. 3, average diameters of the silver nanoparticles are below 15 nm. For smaller nanoparticles (less than about 52 nm for silver), the dipolar polarization contributes the optical response of the colloidal solution with a huge surface scattering process of the conduction conductions by either radiative or non-radiative damping. Therefore, surface scattering of the silver nanoparticles probably caused the broadening of the plasmon bandwidth with time [17].

3.2. Kinetic analysis

When the silver ions reacted with H_3PO_2, reaction rate of the silver ions could be described as

$$-r_{AgNO_3} = -\frac{d[AgNO_3]}{dt} = k[AgNO_3]^a[H_3PO_2]^b = \\ = k\left(\frac{\alpha}{\beta}\right)^a [H_3PO_2]^{a+b} = k_{overall}[H_3PO_2]^n \quad (1)$$

Where $[H_3PO_2]/[AgNO_3] = \beta/\alpha$, n and $k_{overall}$ are the overall reaction order, the overall reaction constant of the silver ions, respectively. For reduction of silver ions in aqueous phosphinic acid containing PVP, overall-reaction order and reaction constant are calculated by Eq. (2) described Half-life analysis. Half-life, $t_{1/2}$, is defined as the reaction time needed to the concentration of silver ions dropped to one-half the original concentration hence we obtain the following [18]

$$t_{1/2} = \frac{(1/2)^{1-n} - 1}{(n-1)k_{overall}}[H_3PO_2]^{1-n} \quad (2)$$

Eq. (2) represents a plot of log $t_{1/2}$ versus log $[H_3PO_2]$ giving a straight line with a slope of 1-n. Overall reaction constant, $k_{overall}$, was determined by the intercept, log $\frac{(1/2)^{1-n}-1}{(n-1)k_{overall}}$. Half-life, $t_{1/2}$, was estimated by the polynomial correlation of the absorbance of the plasmonic peak at 395 nm with time. Depending on different conditions, for all UV-VIS spectra, plasmonic peaks initially appeared at 412 nm – 422 nm gradually blue shifted to 395 nm – 399 nm with time. Thus, we selected the absorbance of UV-VIS spectra at 395 nm as a reference position to calculate the reaction extent of silver ions. Absorbance fluctuations, less than order of 0.01 min^{-1}, were regarded as the completion of the reaction. Correcting for background absorbance of the UV-VIS spectra was carried out by blank sample. For 1:1 – 1:4 of $AgNO_3$ and H_3PO_2 at 25°C, half-life was estimated to be 410.1 min, 126.2 min, 69.4 min. As shown in Fig. 7, plot of ln ($t_{1/2}$) versus ln $[H_3PO_2]$ gives $k_{overall}$ = 0.03 $(mol/L)^{-0.30}min^{-1}$, and n = 1.30, respectively. Rate equation of the silver ions gives

$$-r_{AgNO_3} = -\frac{d[AgNO_3]}{dt} = 0.03[H_3PO_2]^{1.30} \quad (3)$$

Dependence of overall reaction constant, $k_{overall}$, with reaction temperature could be described by a linear Arrhenius law denoted as

$$k_{overall} = Ae^{-\frac{E_{activation}}{RT}} \quad (4)$$

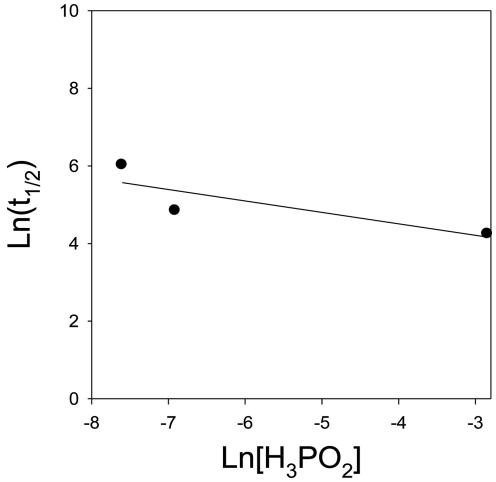

Fig. 7. Plot of ln ($t_{1/2}$) versus ln [H_3PO_2]

Where A is a pre-exponential factor, $E_{activation}$ is the activation energy for the reduction of silver ions in J/mol, R is the gas constant in J/(mol·K), T is the reaction temperature in K. Linear regression of the overall reaction constant against temperature gives the activation energy and pre-exponential factor from Eq. (4). Overall rate constant for each temperature could be calculated from Eq. (2) when we hypothesize the reaction order was not changed. At 25°C, 30°C and 35°C, half-life was estimated to be 410.1, 125.2, and 84.8 min. Hence, overall rate constants were 0.03 $(mol/L)^{-0.30}min^{-1}$, 0.09 $(mol/L)^{-0.30}min^{-1}$ and 0.13 $(mol/L)^{-0.30}min^{-1}$. Plot of overall rate constant versus temperature was given in Fig. 8. The slope was found to be $E_{activation}/R$ = -14522.3. The activation energy, was found to be 120.7 kJ/mol. The endothermic reduction of silver ions occurred in the mixtures of ethanol containing phosphinic acid.

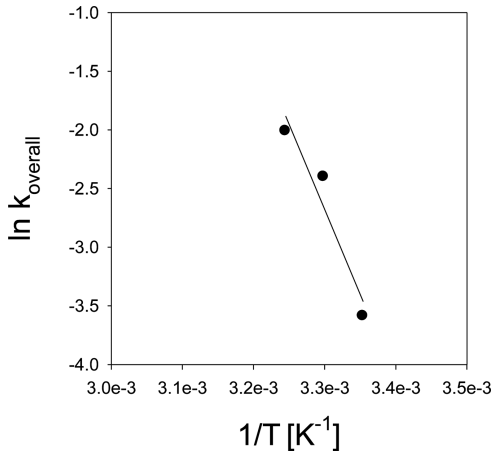

Fig. 8. Plot of ln $k_{overall}$ versus 1/T

4. Conclusions

UV-VIS optical spectra clearly showed the silver nanoparticles were formed in aqueous ethanol containing phosphinic acid with PVP as a stabilizer. X-ray diffraction patterns revealed that the crystalline structure of the silver nanoparticles was face-centered cubic. According to TEM microphotographs, crystalline silver nanoparticles were formed in the range of be 8.5±0.9 nm – 11.3±0.2 nm. By half-life analysis, the reaction order of the silver ions was 1.30 with the activation energy of 120.7 kJ/mol. In the optical spectra of the silver colloids, the resonance peaks slightly shifted toward shorter wavelength with narrowing the line-width. As predicted by Drude's free-electron model, for the very small nanoparticles less than 52 nm, the mean free path limitation causes the blue-shifts of the resonance peaks and the broadening of FWHM with decreasing size because of surface scattering of the conduction electrons.

REFERENCES

[1] Z. Jia, H. Sun, Q. Gu, Colloids and Surfaces A: Physicochem. Eng. Aspects **419**, 174 (2013).
[2] T. Ahmad, I.A. Wani, N. Manzoor, J. Ahmed, A.M. Asiri, Colloids and Surfaces B: Biointerfaces **107**, 227 (2013).
[3] M. Farrag, M. Tschurl, U. Heiz, Chemistry of Materials **25**, 862 (2013).
[4] G.-Q. Lu, J.N. Galata, Preparation of Stable High Concentration Colloidal Metal Particulate System, U.S. Patent application Publication, US 2008/0089839, 2008.
[5] S.J. Son, Y.S. Cho, J.J. Rha, C.J. Choi, J. Kor. Powd. Met. Inst. **20**, 120 (2013).
[6] B. Wiley, T. Herricks, Y. Sun, Y. Xia, Nano Letters **4**, 1733 (2004).
[7] A. Chhatre, P. Solasa, S. Sakle, R. Thaokar, A. Mehra, Colloids and Surfaces A: Physicochemical and Engineering Aspects **404**, 83 (2012).
[8] L. Zhang, Y. Wang, L. Tong, Y. Xia, Langmuir **29**, 15719 (2013).
[9] R. Sankar, A. Karthik, A. Prabu, S. Karthik, K.S. Shivashangari, V. Ravikumar, Colloids and Surfaces B: Biointerfaces **108**, 80 (2013).
[10] H. Wang, X. Qiao, J. Chen, X. Wang, S. Ding, Materials Chemistry and Physics **94**, 449 (2008).
[11] J.S. Kim, J. Ind. Eng. Chem. **13**, 566 (2007).
[12] L.H. Bac, W.H. Gu, J.C. Kim, B.K. Kim, J.S. Kim, J. Kor. Powd. Met. Inst. **19**, 55 (2012).
[13] D. Malina, A. Sobczak-Kupiec, Z. Wzroek, Z. Kowalski, Digest Journal of Nanomaterials and Biostructures **7**, 1527 (2012).
[14] Y. Chaikin, T.A. Benikov, H. Cohen, A. Vaskevich, I. Rubinstein, J. Materials Chemistry C **1**, 3573 (2013).
[15] K.J. Harlieb, M. Saunders, C.L. Raston, Chem. Commun. **21**, 3074 (2009).
[16] G.O. Mallory, J.B. Hajdu, Electroless Plating: Fundamentals and Applications, American Electroplaters and Surface Finishers Society, Inc., New York 1990.
[17] U. Kreibig, M. Vollmer, Optical Properties of Metal Clusters, Berlin 1995.
[18] J.G. Eberhart, E. Levin, Simplified Half-life Methods for the Analysis of Kinetic Data, RIAS Technical Report 88.24, 1988.

Received: 20 November 2014.